



## Fire detection in video sequences using a generic color model

Turgay Çelik\*, Hasan Demirel

*Department of Electrical and Electronic Engineering, Eastern Mediterranean University, Gazimağusa, TRNC, Mersin 10, Turkey*

### ARTICLE INFO

#### Article history:

Received 8 December 2006

Received in revised form

7 May 2008

Accepted 8 May 2008

Available online 7 July 2008

#### Keywords:

Fire detection

Generic color model

Image processing

### ABSTRACT

In this paper, a rule-based generic color model for flame pixel classification is proposed. The proposed algorithm uses YCbCr color space to separate the luminance from the chrominance more effectively than color spaces such as RGB or *rgb*. The performance of the proposed algorithm is tested on two sets of images, one of which contains fire, the other containing fire-like regions. The proposed method achieves up to 99% fire detection rate. The results are compared with two other methods in the literature and the proposed method is shown to have both a higher detection rate and a lower false alarm rate. Furthermore the proposed color model can be used for real-time fire detection in color video sequences, and we also present results for segmentation of fire in video using only the color model proposed in this paper.

© 2008 Elsevier Ltd. All rights reserved.

### 1. Introduction

Fire detection systems are one of the most important components in surveillance systems used to monitor buildings and environment as part of an early warning mechanism that reports preferably the start of fire. Currently, almost all fire detection systems use built-in sensors that primarily depend on the reliability and the positional distribution of the sensors. The sensors should be distributed densely for a high precision fire detector system. In a sensor-based fire detection system, coverage of large areas in outdoor applications is impractical due to the requirement of regular distribution of sensors in close proximity.

Due to the rapid developments in digital camera technology and video processing techniques, there is a big trend to replace conventional fire detection techniques with computer vision-based systems. In general computer vision-based fire detection systems employ three major stages [1–4]. First stage is the flame pixel classification; the second stage is the moving object segmentation, and the last part is the analysis of candidate regions. This analysis is usually based on two figures of merit; shape of the region and the temporal changes of the region.

The fire detection performance depends critically on the performance of the flame pixel classifier which generates seed areas on which the rest of the system operates. The flame pixel classifier is thus required to have a very high detection rate and preferably a low false alarm rate. There exist few algorithms which directly deal with the flame pixel classification in the literature. The flame pixel classification can be considered both in

grayscale and color video sequences. Krull et al. [5] used low-cost CCD cameras to detect fires in the cargo bay of long range passenger aircraft. The method uses statistical features, based on grayscale video frames, including mean pixel intensity, standard deviation, and second-order moments, along with non-image features such as humidity and temperature to detect fire in the cargo compartment. The system is commercially used in parallel to standard smoke detectors to reduce the false alarms caused by the smoke detectors. The system also provides visual inspection capability which helps the aircraft crew to confirm the presence or absence of fire. However, the statistical image features are not considered to be used as part of a standalone fire detection system. Most of the works on flame pixel classification in color video sequences are rule based. Chen et al. [1] used raw R, G, and B information and developed a set of rules to classify the flame pixels. Instead of using the rule-based color model as in Chen et al., Töreyin et al. [2] used a mixture of Gaussians in *RGB* space which is obtained from a training set of flame pixels. In a recent paper, the authors employed Chen's flame pixel classification method along with a motion information and Markov field modeling of the flame flicker process [3]. Marbach et al. [6] used YUV color model for the representation of video data, where time derivative of luminance component *Y* was used to declare the candidate fire pixels and the Chrominance components *U* and *V* were used to classify the candidate pixels to be in the fire sector or not. In addition to luminance and chrominance they have incorporated motion into their work. They report that their algorithm detects less than one false alarm per week; however, they do not mention the number of tests conducted. Homg et al. [7] used HSI color model to roughly segment the fire-like regions for brighter and darker environments. Initial segmentation is followed by removing lower intensity and lower saturation pixels

\* Corresponding author. Tel.: +90 392 6301436; fax: +90 392 3650240.  
E-mail address: [turgay.celik@emu.edu.tr](mailto:turgay.celik@emu.edu.tr) (T. Çelik).

in order to get rid of the spurious fire-like regions such as smoke. They also introduced a metric based on binary contour difference images to measure the burning degree of fire flames into classes such as “no fire”, “small”, “medium” and “big” fires. They report 96.94% detection rate, together with results including false positives and false negatives for their algorithms. However, there

is no attempt to reduce the false positives and false negatives by changing their threshold values. Celik et al. [4] used normalized *RGB* (*rgb*) values for a generic color model for the flame. The normalized *RGB* is proposed in order to alleviate the effects of changing illumination. The generic model is obtained using statistical analysis carried out in *r-g*, *r-b*, and *g-b* planes. Due to

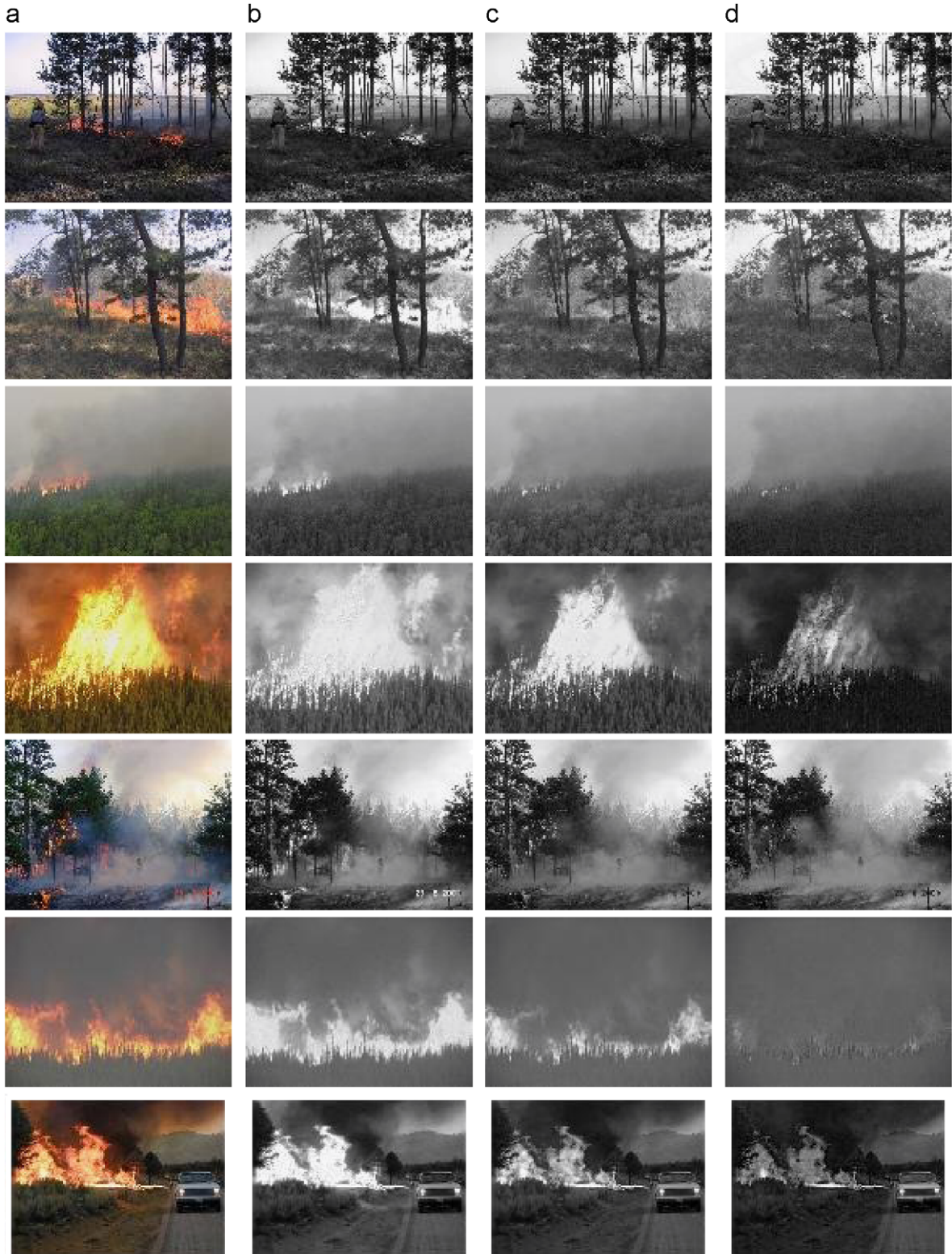


**Fig. 1.** Original *RGB* color images in column (a), and *R*, *G*, and *B* channels in columns (b)–(d), respectively.

the distribution nature of the sample fire pixels in each plane, three lines are used to specify a triangular region representing the region of interest for the fire pixels. Therefore, triangular regions in respective  $r-g$ ,  $r-b$ , and  $g-b$  planes are used to classify a pixel. A pixel is declared to be a fire pixel if it falls into three of the triangular regions in  $r-g$ ,  $r-b$ , and  $g-b$  planes. Even though normalized  $RGB$  color space overcomes to some extent the effects of variations in illumination, further improvement can be achieved if one uses  $YCbCr$  color space which makes it possible to separate luminance/illumination from chrominance.

In this paper we propose to use the  $YCbCr$  color space to construct a generic chrominance model for flame pixel classification. In addition to translating the rules developed in the  $RGB$  and normalized  $rgb$  to  $YCbCr$  color space, new rules are developed in  $YCbCr$  color space which further alleviate the harmful effects of changing illumination and improves detection performance. The flame pixel classification rates of the proposed system with new rules and new generic chrominance model is compared with the previously introduced flame pixel classification models. The proposed model gives 99.0% correct flame pixel classification rate with a 31.5% false alarm rate. This is a significant improvement over other methods used in the literature.

## 2. Classification of flame pixels

Each digital color image is composed of three color planes: red, green, and blue ( $R$ ,  $G$ , and  $B$ ). Each color plane represents a color-receptor in human eye working on different wavelength. The combination of  $RGB$  color planes gives ability to devices to represent a color in digital environment. Each color plane is quantized into discrete levels. Generally 256 (8 bits per color plane) quantization levels are used for each plane, for instance white is represented by  $(R, G, B) = (255, 255, 255)$  and black is represented by  $(R, G, B) = (0, 0, 0)$ . A color image consists of pixels, where each pixel is represented by spatial location in rectangular grid  $(x, y)$ , and a color vector  $(R(x, y), G(x, y), B(x, y))$  corresponding to spatial location  $(x, y)$ . Each pixel in a color image containing a

**Table 1**  
Mean values of  $R$ ,  $G$ , and  $B$  planes of fire regions for images given in Fig. 2

Row index in Fig. 2	Mean of $R$	Mean of $G$	Mean of $B$
1	218	137	97
2	152	84	75
3	211	158	105



**Fig. 2.** Original  $RGB$  images are given in column (a) and corresponding fire regions, manually labeled with green color, are given in column (b).

fire blob (region containing fire), the value of Red channel is greater than the Green channel, and the value of Green channel is greater than the value of Blue channel for the spatial location. Furthermore, the flame color has high saturation in Red channel

[1,4]. For instance in Fig. 1 column (a) shows samples of digital color images, and columns (b)–(d) show R, G, and B color planes (channels), respectively. It can be noticed from Fig. 1 that for the fire regions, R channel has higher intensity values than the G

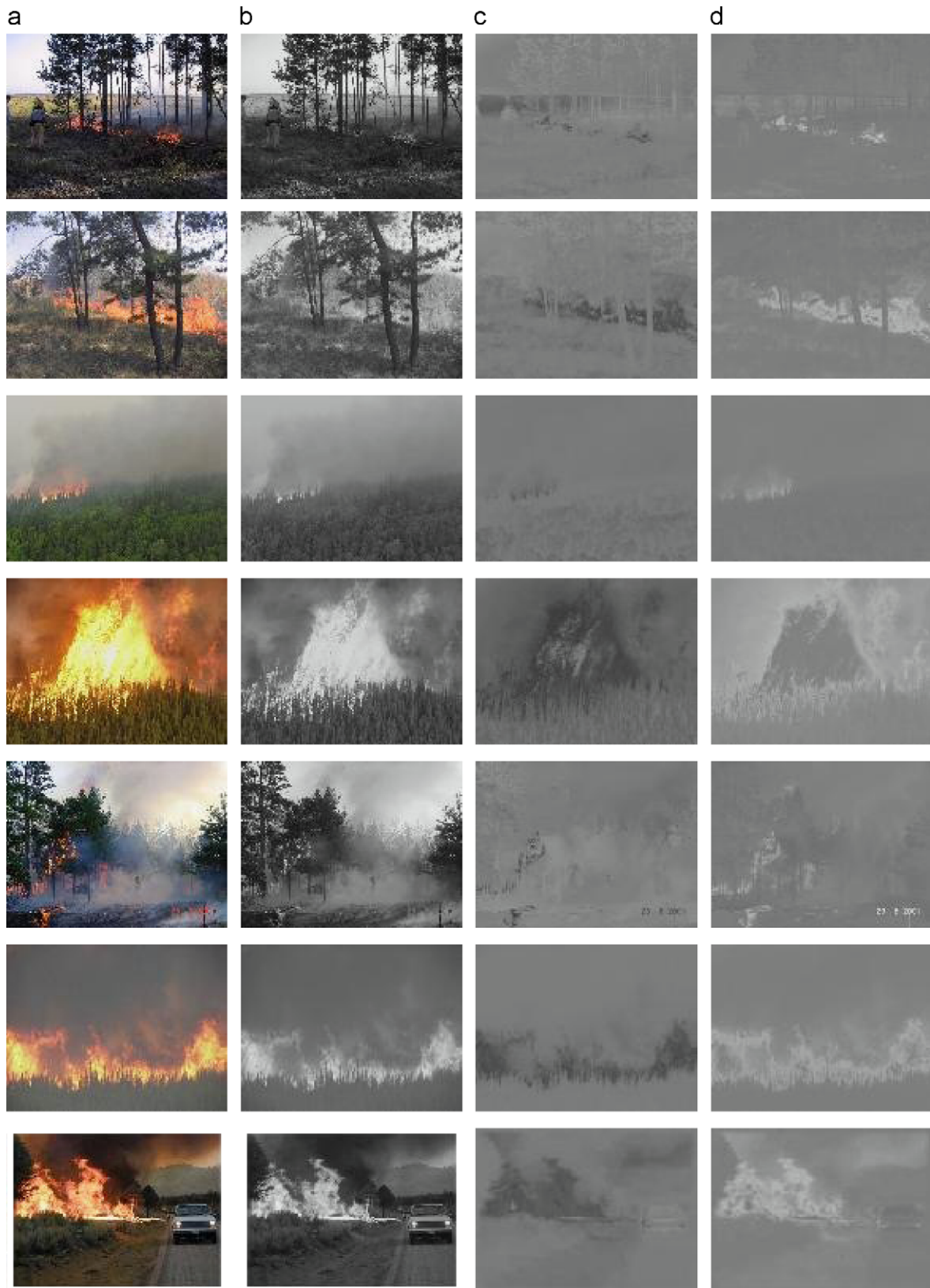


**Fig. 3.** RGB color images in column (a) and its Y, Cb, and Cr channels in columns (b)–(d), respectively.

channel, and  $G$  channel has higher intensity values than the  $B$  channel.

In order to explain this idea better, we picked sample images from Fig. 1(a), and segmented its fire pixels as shown in Fig. 2(b) with green color. Then we calculate mean values of  $R$ ,  $G$ , and  $B$  planes in the segmented fire regions of the original images. The results are given in Table 1 for the images given in Fig. 2. It is clear that, on the average, the fire pixels show the characteristics that their  $R$  intensity value is greater than  $G$  and  $G$  intensity value is greater than the  $B$ .

Even though  $RGB$  color space can be used for pixel classification, it has disadvantages of illumination dependence. It means that if the illumination of image changes, the fire pixel classification rules can not perform well. Furthermore, it is not possible to separate a pixel's value into intensity and chrominance. The chrominance can be used in modeling color of fire rather than modeling its intensity. This gives more robust representation for fire pixels. So it is needed to transform  $RGB$  color space to one of the color spaces where the separation between intensity and chrominance is more discriminate. Because of the linear conversion between  $RGB$  and  $YCbCr$  color spaces, we use  $YCbCr$  color space to model fire pixels. The conversion from  $RGB$  to  $YCbCr$  color space is formulated as follows [8]:

$$\begin{bmatrix} Y \\ Cb \\ Cr \end{bmatrix} = \begin{bmatrix} 0.2568 & 0.5041 & 0.0979 \\ -0.1482 & -0.2910 & 0.4392 \\ 0.4392 & -0.3678 & -0.0714 \end{bmatrix} \begin{bmatrix} R \\ G \\ B \end{bmatrix} + \begin{bmatrix} 16 \\ 128 \\ 128 \end{bmatrix} \quad (1)$$

**Table 2**  
Mean values of  $Y$ ,  $Cb$ , and  $Cr$  planes of fire regions of images given in Fig. 2

Row index in Fig. 2	Mean of $Y$	Mean of $Cb$	Mean of $Cr$
1	151	98	166
2	125	114	158
3	160	97	155

where  $Y$  is luminance,  $Cb$  and  $Cr$  are ChrominanceBlue and ChrominanceRed components, respectively. The range of  $Y$  is [16 235],  $Cb$  and  $Cr$  are equal to [16 240].

For a given image, one can define the mean values of the three components in  $YCbCr$  color space as

$$\begin{aligned} Y_{\text{mean}} &= \frac{1}{K} \sum_{i=1}^K Y(x_i, y_i) \\ Cb_{\text{mean}} &= \frac{1}{K} \sum_{i=1}^K Cb(x_i, y_i) \\ Cr_{\text{mean}} &= \frac{1}{K} \sum_{i=1}^K Cr(x_i, y_i) \end{aligned} \quad (2)$$

where  $(x_i, y_i)$  is the spatial location of the pixel,  $Y_{\text{mean}}$ ,  $Cb_{\text{mean}}$ , and  $Cr_{\text{mean}}$  are the mean values of luminance, ChrominanceBlue, and ChrominanceRed channels of pixels, and  $K$  is the total number of pixels in image.

The rules defined for  $RGB$  color space, i.e.  $R \geq G \geq B$ , and  $R \geq R_{\text{mean}}$  [4,1], can be translated into  $YCbCr$  space as

$$Y(x, y) > Cb(x, y) \quad (3)$$

$$Cr(x, y) > Cb(x, y) \quad (4)$$

where  $Y(x, y)$ ,  $Cb(x, y)$ , and  $Cr(x, y)$  are luminance, ChrominanceBlue and ChrominanceRed values at the spatial location  $(x, y)$ . Eqs. (3) and (4) imply, respectively, that flame luminance should be greater than ChrominanceBlue and ChrominanceRed should be greater than the ChrominanceBlue. Eqs. (3) and (4) can be interpreted to be a consequence of the fact that the flame has saturation in red color channel ( $R$ ). In Fig. 3, we show the  $RGB$  images and its corresponding  $Y$ ,  $Cb$ , and  $Cr$  channel responses for the images shown in Fig. 1. The validity of Eqs. (3) and (4) can easily been observed for fire regions.

Similar to Table 1, we picked sample images from Fig. 1(a), and segmented its fire pixels as shown in Fig. 2(b). Then we calculate mean values of  $Y$ ,  $Cb$ , and  $Cr$  planes in the segmented fire regions



**Fig. 4.**  $RGB$  input image and its  $Y$ ,  $Cb$ , and  $Cr$  channels: (a) original  $RGB$  image, (b)  $Y$  channel, (c)  $Cb$  channel, and (d)  $Cr$  channel.

of the original images. The results are given in Table 2 for the images given in Fig. 2. It is clear that, on the average, the fire pixels shows the characteristics that their Y color value is greater than  $Cb$  color value and  $Cr$  color value is greater than the  $Cb$  color value.

Besides these two rules (Eqs. (3) and (4)), since the flame region is generally the brightest region in the observed scene, the mean values of the three channels, in the overall image  $Y_{\text{mean}}$ ,  $Cb_{\text{mean}}$ , and  $Cr_{\text{mean}}$  contain valuable information. For the flame region the value of the Y component is bigger than the mean Y component of the overall image while the value of  $Cb$  component is in general smaller than the mean  $Cb$  value of the overall image. Furthermore, the  $Cr$  component of the flame region is bigger than the mean  $Cr$  component. These observations which are verified over countless experiments with images containing fire regions are formulated as the following rule:

$$F(x,y) = \begin{cases} 1, & \text{if } Y(x,y) > Y_{\text{mean}}, Cb(x,y) < Cb_{\text{mean}}, Cr(x,y) > Cr_{\text{mean}} \\ 0, & \text{otherwise} \end{cases} \quad (5)$$

where  $F(x, y)$  indicates that any pixel which satisfies condition given in Eq. (5) is labeled as fire pixel.

Fig. 4 shows the three channels for a representative image containing fire in more detail. The rule in (5) can be easily verified. It can easily be observed from the representative fire image (Fig. 4(c) and (d)) that there is a significant difference between the  $Cb$  and  $Cr$  components of the flame pixels. The  $Cb$  component is predominantly “black” while the  $Cr$  component is predominantly “white”. This fact is formulated as a rule as follows:

$$F_{\tau}(x,y) = \begin{cases} 1, & \text{if } |Cb(x,y) - Cr(x,y)| \geq \tau \\ 0, & \text{otherwise} \end{cases} \quad (6)$$

where  $\tau$  is a constant.

The value of  $\tau$  is determined using a receiver operating characteristics (ROC) [9] analysis of Eq. (6) on an image set

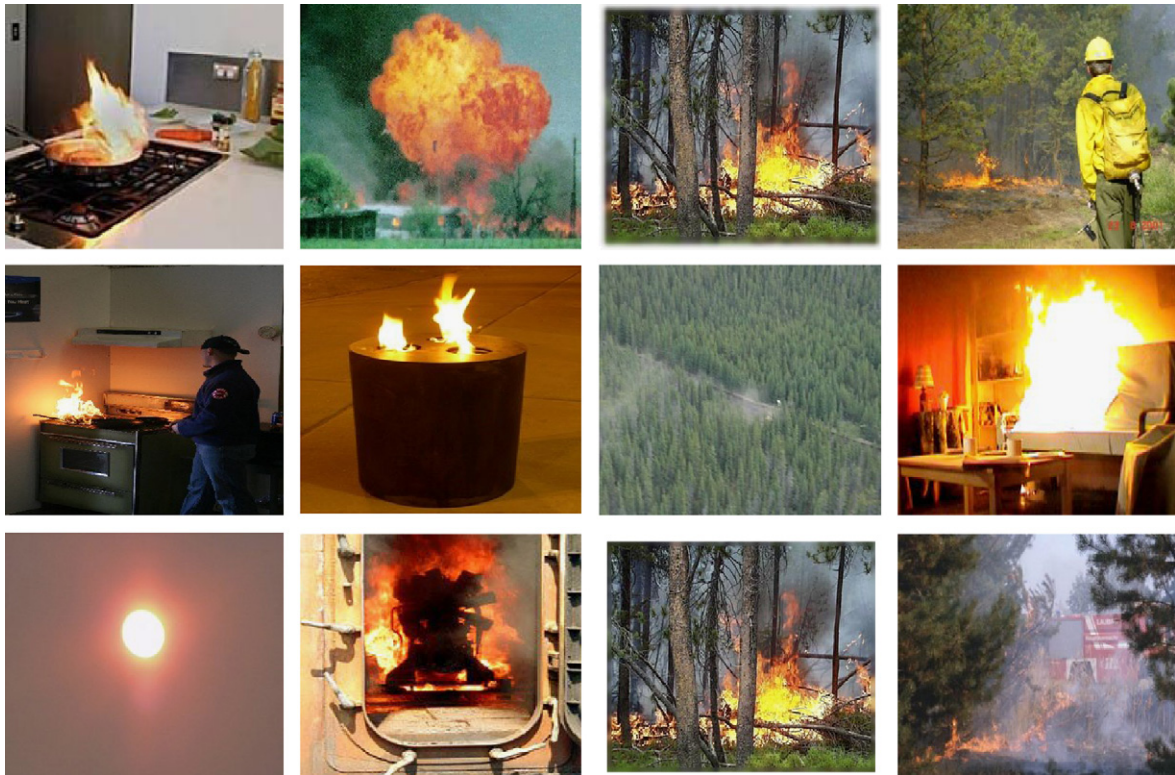


Fig. 5. Samples from set of images used in ROC curve analysis.

consisting of 1000 images. Fig. 5 shows a few samples from this set. Note that in Fig. 5, there are a variety of images including ones with changing illumination and lighting. Furthermore, the images are selected so that fire-like colored objects are also included in the set. For instance the Sun in the image that produces fire-like color. There are some images in the set which do not contain any fire. The image set consists of random images collected from the internet. Images are from both indoor and outdoor environments.

The ROC curve for the image set is given in Fig. 6 where hand segmented fire images are used in order to create the ROC curve. The rules (2) through (6) are applied to hand segmented fire

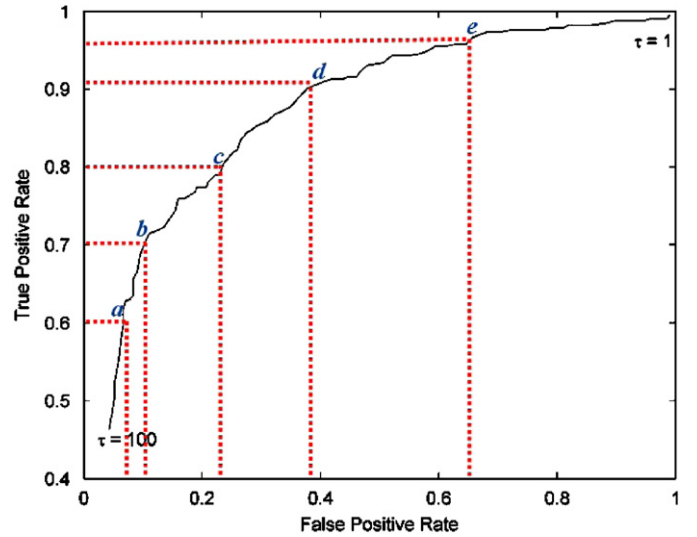


Fig. 6. Receiver operating characteristics for  $\tau$ .

images with different values of  $\tau$  changing from 1 to 100. For each value of  $\tau$ , we calculate corresponding true and false positive rates on the image set and tabulate it. The true positive is defined as the decision when an image contains a fire, and false positive is defined as the decision when an image contains no fire but classified as having fire. The ROC curve consists of 100 data points corresponding to different  $\tau$  values and some of them are labeled in Fig. 6 with blue letters, i.e. *a*–*e*. For each point in the ROC curve there are three values; true positive rate, false positive rate, and  $\tau$ . For instance, for the point labeled with *a*, the true positive rate is 60%, false positive rate is 6% and corresponding  $\tau$  is 96. Using the ROC curve, different values of  $\tau$  can be selected with respect to required true positive and false positive rates.

Since fire detection systems should not miss any fire alarm, the value of  $\tau$  should be selected so that systems true positive rate is high enough. It is clear from Fig. 6 that, high positive rate means

that high false positive rate. Using this tradeoff, in our experiments the value of  $\tau$  is picked such that the detection rate is over 90% and false alarm rate is less than 40% (point *d*) which corresponds to  $\tau = 40$ .

In addition to the above rules a statistical analysis of chrominance information in flame pixels over a larger set of images is performed. For this purpose a set of 1000 images, containing fire at different resolutions are collected from the Internet. Samples from this set are shown in Fig. 7. The collected set of images has a wide range of illumination and camera effects. The fire regions in the 1000 images are manually segmented and the histogram of a total of 16,309,070 pixels is created in the  $Cb$ – $Cr$  chrominance plane. Fig. 8 shows the distribution of flame pixels in  $Cb$ – $Cr$  plane. The area containing flame pixels in  $Cb$ – $Cr$  plane can be modeled using intersections of three polynomials denoted by  $fu(Cr)$ ,  $fl(Cr)$ , and  $fd(Cr)$ . The



**Fig. 7.** Samples from set of images used in extracting chrominance model for fire-pixels.

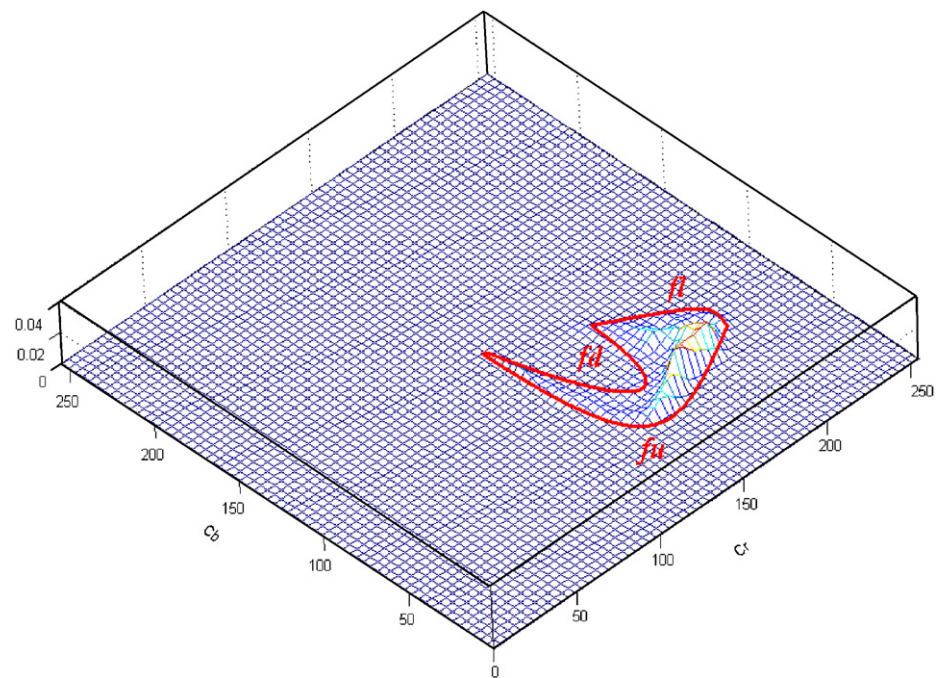


**Fig. 8.** 3-D distribution of hand labeled flame pixels in  $Cb$ – $Cr$  color plane and three polynomials,  $fu(Cr)$ ,  $fl(Cr)$ , and  $fd(Cr)$ , bounding the flame region.



**Fig. 9.** Fire detection in a still image: (a) original image, (b) fire segmentation using only (3), (c) fire segmentation using only (4), (d) fire segmentation using only (5), (e) fire segmentation using only (6), (f) fire segmentation using only (8), (g) fire segmentation using combination (3)–(6) and (8), and (h) segmented color image which consists of fire.

equations for the polynomials are derived using a least-square estimation technique [10]:

$$\begin{aligned} fu(Cr) = & -2.6 \times 10^{-10} Cr^7 + 3.3 \times 10^{-7} Cr^6 \\ & - 1.7 \times 10^{-4} Cr^5 + 5.16 \times 10^{-2} Cr^4 - 9.10 \times Cr^3 \\ & + 9.60 \times 10^2 Cr^2 - 5.60 \times 10^4 Cr + 1.40 \times 10^6 \\ fl(Cr) = & -6.77 \times 10^{-8} Cr^5 + 5.50 \times 10^{-5} Cr^4 \\ & - 1.76 \times 10^{-2} Cr^3 + 2.78 Cr^2 \\ & - 2.15 \times 10^2 Cr + 6.62 \times 10^3 \\ fd(Cr) = & 1.81 \times 10^{-4} Cr^4 - 1.02 \times 10^{-1} Cr^3 + 2.17 \times 10 Cr^2 \\ & - 2.05 \times 10^3 Cr + 7.29 \times 10^4 \end{aligned} \quad (7)$$

The region bounded by the three polynomials is depicted in Fig. 8. The boundaries of the region which correspond to the polynomials are shown in red. Once this region is obtained, it is easy to define another rule for classifying the flame pixel. We formulate this in Eq. (8) as follows:

$$F_{CbCr}(x, y) = \begin{cases} 1, & \text{if } Cb(x, y) \geq fu(Cr(x, y)) \cap Cb(x, y) \leq fd(Cr(x, y)) \cap Cb(x, y) \leq fl(Cr(x, y)) \\ 0, & \text{otherwise} \end{cases} \quad (8)$$

where  $F_{CbCr}(x, y)$  shows whether corresponding pixel at spatial location  $(x, y)$  falls into region defined by boundaries formulated in Eq. (7) with 1 indicating that it is included in this region and 0 indicating that it is not included and  $\cap$  is the binary AND operator.

With the derived set of rules in the  $YCbCr$  color space given in Eqs. (3)–(6) and (8), one can classify whether a given pixel is a flame pixel or not. The overall segmentation process is illustrated

**Table 3**  
Performance of the proposed algorithm compared with two similar algorithms in the literature

Color model	Detection rate in fire set	False alarm rate in non-fire set
RGB [1]	0.939	0.664
rgb [4]	0.970	0.584
YCbCr, proposed	0.990	0.315

in Fig. 9 in a step-by-step manner. As can be seen from Fig. 9, each rule produces false alarms, but their overall combination produces the result which is convenient in identifying fire regions in corresponding color image.

### 3. Performance analysis

The performance of the proposed flame pixel classifier model is compared with the models defined in [1,4]. The model defined by Chen et al. [1] uses raw RGB values, and rules defined over RGB space. On the other hand, the model defined by Celik et al. [4] uses  $YCbCr$  values.

Performance analysis is carried out using a set of 751 color images of size  $256 \times 256$  which are totally different from the sets used in creating the fire color model. The set consists of 332 images which contain flame, and the rest is a collection of images which do not contain any flame. It should be noted that this set may contain flame-like objects such as the Sun, a red rose, etc.



**Fig. 10.** Demonstration of fire segmentation in four different video sequences (a–d) with frame numbers of 1, 11, 21, 31, 41, 51, 61, and 71 are selected for visualization.



**Fig. 10.** (Continued)

In Table 3, we have tabulated flame detection results with false alarm rates. It is clear that the proposed model outperforms the model which uses *rgb* values proposed by Celik et al. both in detection rates and false alarm rate. The proposed model has better performance than the model proposed by Chen et al. which operates in *RGB* color space.

The performance improvement is expected since *YCbCr* color space has the ability of discriminating luminance from chrominance information. Since the chrominance dominantly represents information without effect of luminance, the chrominance-based rules and the color model defined in the chrominance plane are more descriptive for flame behavior.

We have demonstrated fire segmentation for outdoor uncontrolled environment using four different video sequences from Wildland Fire Operations Research Group in Canada [11]. The sequences consist of views of different forest fire scenes recorded from a helicopter. The segmentation results using the proposed generic color model are shown in Fig. 10. Each video sequence consists of frames recorded consecutively. The model defined in this paper is applied to each frame of the video sequences. Each frame and its corresponding binary map showing fire pixels is shown in Fig. 10 where it is clear that the proposed color model robustly detects fire regions in the given video sequences.

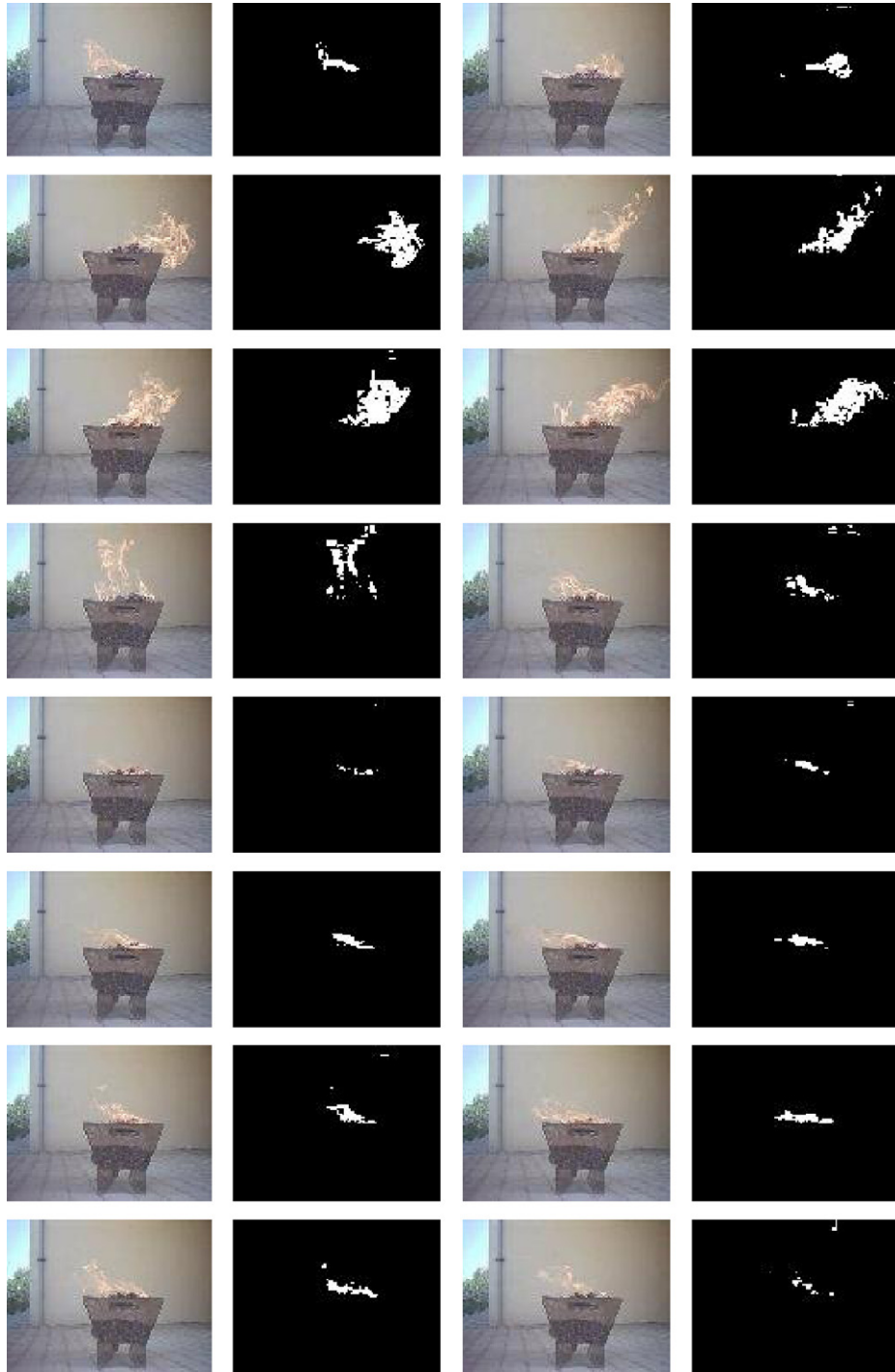


**Fig. 11.** Demonstration of fire segmentation in an indoor video sequence collected from Celik et al. [4].

We also demonstrated fire segmentation for indoor controlled environment using a video sequence from Töreyin et al. [3]. The video sequence consists of fire in a controlled environment where the fire spread is changing with time. The fire segmentation results are presented in Fig. 11. It is clearly noticeable from Fig. 11 that, the proposed color model robustly detects fire regions in the given video sequence.

#### 4. Computational complexity

In order to perform in real-time, the proposed model should be cheap in computational power. The computational complexity analysis of the proposed algorithm is introduced in this section.

Let us assume that the size of input *RGB* image is  $H \times W$ , where *H* and *W* are height and width of the input *RGB* image, respectively. We evaluate computational complexity of the proposed algorithm by finding number of *additions/subtractions* (*adds/subs*), *divisions/multiplications* (*divs/muls*), and *comparisons* (*comps*).

The first stage in the algorithm is the conversion from *RGB* to *YCbCr* color space. For each pixel at spatial location  $(x,y)$ , the conversion from *RGB* to *YCbCr* using Eq. (1) requires 9 *adds/subs* and 9 *divs/muls*. Total number of operations required to convert all pixels from *RGB* to *YCbCr* is 9*HW* *adds/subs* and 9*HW* *divs/muls*. After converting from *RGB* to *YCbCr* color space, the next stage is calculation of statistical parameters given in Eq. (2). Eq. (2) requires 3(*HW*-1) *adds/subs* and 3 *divs/muls*. Eqs. (3) and (4) are simple binary comparisons, and each of them requires *HW* *comps*. Eq. (5) uses statistics derived from Eq. (2) to make simple binary comparisons and it requires 3*HW* *comps*. The absolute value in Eq. (6) is actually a comparison to check whether or not the number is greater than 0. By using this information Eq. (6) requires *HW* *comps* and 2*HW* *comps*.

The analytic equation defined in Eq. (7) requires high order numerical calculations. Since the *Cr* is an integer numeric variable in the range of [16 240], we use a lookup table. The lookup table consists of values of analytic functions defined in Eq. (7) for each value of *Cr*. Since we are using a lookup table for the Eq. (7), we do not need any arithmetic operation for it. The created lookup table for Eq. (7) is used in Eq. (8). The binary AND operator in Eq. (8) is simply a comparison to check whether the binary values input to AND operator are all binary 1 or 0. Using this information, total number of operations for Eq. (8) is 6*HW* *comps*.

The final classification whether a given pixel is a flame pixel or not is done by combining results from Eqs. (3)–(6) and Eq. (8). This operation is done by applying binary AND to results from Eqs. (3)–(6) and Eq. (8). Therefore, the final stage requires 5*HW* *comps*.

Total number of arithmetic operations required for the proposed method is tabulated in Table 4. The total number of arithmetic operations are 13*HW*-1 *adds/subs*, 9*HW*+3 *divs/muls*, and 18*HW* *comps*. It is clear that the number of arithmetic operations is linear with image size and hence the proposed algorithm is very cheap in computational complexity.

#### 5. Conclusions

In this paper, a generic color model for flame pixel classification is proposed. The proposed color model uses *YCbCr* color space, which is better in discriminating the luminance from the

**Table 4**  
Arithmetic operations used in proposed method

Equation	adds/subs	divs/muls	comps
(1)	9 <i>HW</i>	9 <i>HW</i>	–
(2)	3( <i>HW</i> -1)	3	–
(3)	–	–	<i>HW</i>
(4)	–	–	<i>HW</i>
(5)	–	–	3 <i>HW</i>
(6)	<i>HW</i>	2 <i>HW</i>	–
(7)	–	–	–
(8)	–	–	6 <i>HW</i>
Final classification	5 <i>HW</i>		
Total operations	13 <i>HW</i> -1	9 <i>HW</i> +3	18 <i>HW</i>

chrominance, hence is more robust to the illumination changes than *RGB* or *rgb* color spaces. The performance of the proposed color model is tested on two sets of images; one containing fire and the other containing fire-like regions. The proposed color model achieves 99.0% flame detection rate and 31.5% false alarm rate. The results are compared with two other methods in the literature and the performance improvement of the proposed method both in correct fire detection rate and false alarm rate is demonstrated.

The number of arithmetic operations for the proposed color model is linear with image size and algorithm is very cheap in computational complexity. This makes it suitable for the real-time applications.

The proposed color model can be used in fire detection in video sequences. We have shown that the proposed algorithm performs well in segmenting fire regions in video sequences. In our future work, we will make the time analysis of fire regions in video sequence by measuring spread in the fire regions. Furthermore, the flicker nature of fire will be considered as a future work.

#### References

- [1] T. Chen, P. Wu, Y. Chiou, An early fire-detection method based on image processing, in: Proceedings of IEEE International on Image Processing, 2004, pp. 1707–1710.
- [2] B.U. Töreyin, Y. Dedeoğlu, A.E. Çetin, Flame detection in video using hidden Markov models, in: Proceedings of IEEE International Conference on Image Processing, 2005, pp. 1230–1233.
- [3] B.U. Töreyin, Y. Dedeoğlu, U. Güdükbay, A.E. Çetin, Computer vision based method for real-time fire and flame detection, Pattern Recognition Lett. 27 (1) (2006) 49–58.
- [4] T. Çelik, H. Demirel, H. Ozkaramanlı, Automatic fire detection in video sequences, in: Proceedings of European Signal Processing Conference (EUSIPCO 2006), Florence, Italy, September 2006.
- [5] W. Krull, I. Willms, R.R. Zakrzewski, M. Sadok, J. Shirer, B. Zeliff, Design and test methods for a video-based cargo fire verification system for commercial aircraft, Fire Saf. J. 41 (4) (2006) 290–300.
- [6] G. Marbach, M. Loepfe, T. Bruppacher, An image processing technique for fire detection in video images, Fire Saf. J. 41 (4) (2006) 285–289.
- [7] Wen-Bing Homg, Jim-Wen Peng, Chih-Yuan Chen, A new image-based real-time flame detection method using color analysis, in: Proceedings of IEEE Networking, Sensing and Control, ICNSC, 2005, pp. 100–105.
- [8] C.A. Poynton, A Technical Introduction to Digital Video, Wiley, New York, 1996.
- [9] D.M. Green, J.M. Swets, Signal Detection Theory and Psychophysics, Wiley, New York, 1966.
- [10] J.H. Mathews, K.D. Fink, Numerical Methods using MATLAB, Prentice-Hall, Englewood Cliffs, NJ, 1999.
- [11] Wildland Fire Operations Research Group, Retrieved August 11, 2006, from <<http://fire.feric.ca/index.htm>>.